Quantum reflections and inelastic scattering of electrons in semiconductor heterostructures

J. F. Müller,* A. F. J. Levi, and S. Schmitt-Rink
AT&T Bell Laboratories, Murray Hill, New Jersey 07974-2070
(Received 16 March 1988)

We study the contribution of polar optic phonons to the inelastic scattering rate for the two distinct cases of a nonequilibrium electron initially moving parallel and perpendicular to semiconductor heterojunctions. Quantum mechanical reflections from the abrupt change in potential at the heterointerface are found to change the inelastic scattering rate by spatially separating initial and final electron wave functions. In this paper we explore this effect for typical heterojunction geometries and discuss the influence of the phenomenon on the performance of devices, such as field-effect and unipolar hot-electron transistors.

I. INTRODUCTION

Currently there is little understanding of the dynamics of nonequilibrium electrons moving in the abruptly changing potentials of semiconductor heterojunctions. However, knowledge of electron scattering in such structures is of fundamental interest and has technological significance by, for example, assisting in the design of hot-electron transistors.[1] In the past, attempts have been made to calculate polar-optic-phonon scattering rates, $1/\tau$, for initial electron motion parallel to a heterojunction quantum well.[2] Recently, we reported calculations of $1/\tau$ for initial electron motion perpendicular to semiconductor heterojunctions.[3] Our work demonstrated, for the first time, the important role *elastic* scattering from abrupt changes in potential has in determining total *inelastic* scattering rates. We found a reduction in $1/\tau$ compared to the bulk value for a limited range of electron energies. This effect is related to spatial separation of initial and final electron wave functions on either side of the heterojunction caused by quantum mechanical reflection at the interface. In this paper we present results of a detailed study of this and related phenomena. Ultimately, we wish to understand the nonequilibrium transport properties of various heterojunctions devices. Here, however, we shall restrict ourselves to determination of $1/\tau$ for typical heterojunction geometries and discuss the influence our findings may have on the transport problem.

II. ELECTRON DYNAMICS IN HETEROJUNCTION GEOMETRIES

A. Calculation of the wave functions

In Fig. 1 we show a schematic diagram of the conduction-band edge of a typical hot-electron transistor.[1,3] For simplicity, the potential energies in the emitter, base, and collector region, $U_1, U_2 = 0$ and U_3, respectively, are assumed to be constant. In addition, we only consider the case for which $U_1 \geq U_3 \geq U_2$. Electrons traversing this structure suffer elastic scattering at the abrupt interfaces at $z=0$ and $z=z_2$. We aim to explore the interplay between this quantum mechanical reflection at the transistor's heterointerfaces and inelastic scattering by emission of polar-optic phonons as electrons traverse the device. In order to find the inelastic scattering rate, it is necessary to calculate the eigenstates of the potential depicted in Fig. 1. One may then proceed and use second-order perturbation theory to derive the lifetime of these states due to phonon emission.

The wave functions are calculated by solving the Schrödinger equation for an electron moving in the potential shown in Fig. 1. Since the momentum parallel to the interfaces, $\mathbf{k}_\parallel$, is conserved, the wave functions may be written in the form

$$\psi_{n,\mathbf{k}_\parallel}(\mathbf{r}_\parallel, z) \propto e^{i\mathbf{k}_\parallel \cdot \mathbf{r}_\parallel} \phi_n(z) , \tag{1}$$

where ϕ_n describes the transverse motion and n is the

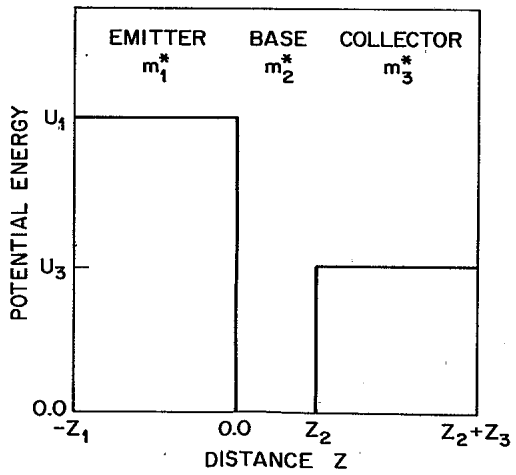

FIG. 1. Schematic potential energy diagram of a double-heterojunction hot-electron transistor. An electron traversing the structure experiences a potential U_1 in the emitter, U_2 in the base, and U_3 in the collector. The emitter, base, and collector are of width z_1, z_2, and z_3, respectively. The effective electron masses are m_1^*, m_2^*, and m_3^*.

subband index. In general, we wish to distinguish between the effective electron masses m_j^* $(j=1,2,3)$ in the different transistor regions. In this case, however, the kinetic energy parallel to the interfaces $(\hbar^2 k_\parallel^2/2m_j^*)$ is not conserved and ϕ_n will depend on $k_\parallel$ also. Since we are interested in the effects of scattering on the transverse motion, we avoid this complication by choosing different transverse masses $m_{j\perp}^* \equiv m_j^*$ but equal parallel masses $m_{j\parallel}^* = m_2^*$. The one-dimensional Schrödinger equation for ϕ_n then reads

$$\left[-\frac{\hbar^2}{2m_j^*}\frac{d^2}{dz^2}+U_j\right]\phi_{nj}(z)=E_n\phi_{nj}(z), \quad j=1,2,3 , \tag{2}$$

where E_n is the transverse energy. The total energy is

$$E=E_n+\frac{\hbar^2 k_\parallel^2}{2m_2^*} . \tag{3}$$

Equation (2) is solved by using the ansatz

$$\phi_{jn}(z)=A_{nj}e^{ik_{nj}z}+B_{nj}e^{-ik_{nj}z} , \tag{4}$$

where

$$k_{nj}=\frac{1}{\hbar}[2m_j^*(E_n-U_j)]^{1/2} \tag{5}$$

is the transverse wave number. The energy spectrum $\{E_n\}$ and the amplitudes $\{A_{nj},B_{nj}\}$ are determined by using the boundary conditions

$$\phi_n(-z_1)=\phi_n(z_2+z_3)=0 , \tag{6}$$

$$\phi_{n1}(0)=\phi_{n2}(0) , \tag{7}$$

$$\phi_{n2}(z_2)=\phi_{n3}(z_2) , \tag{8}$$

$$\frac{1}{m_1^*}\frac{d\phi_{n1}}{dz}(0)=\frac{1}{m_2^*}\frac{d\phi_{n2}}{dz}(0) , \tag{9}$$

$$\frac{1}{m_2^*}\frac{d\phi_{n2}}{dz}(z_2)=\frac{1}{m_3^*}\frac{d\phi_{n3}}{dz}(z_2) , \tag{10}$$

and

$$\int_{-z_1}^{z_2+z_3} dz\,|\phi_n(z)|^2=1 . \tag{11}$$

The normalization of the wave functions is conveniently achieved by placing infinite potential barriers at distances $-z_1$ and (z_2+z_3) from the base region. The energy spectrum is finally obtained from Eqs. (6)–(11) by solving for the zeros of a function which depends on the transverse electron wave numbers in each region. This equation for the transverse energies, $E_n=(\hbar^2 k_{n2}^2/2m_2^*)$, is

$$\begin{aligned}0&=f(k_2)\\&=\frac{a_2}{a_1}\tan(k_1z_1)+\tan(k_2z_2)+\frac{a_2}{a_3}\tan(k_3z_3)\\&\quad-\left[\frac{a_2}{a_1}\tan(k_1z_1)\right][\tan(k_2z_2)]\left[\frac{a_2}{a_3}\tan(k_3z_3)\right] ,\end{aligned} \tag{12}$$

where the transverse velocities are given by $a_j=(\hbar k_j)/m_j^*$. For $z_1,z_3 \gg z_2$, one has two quasi-continua of scattering states for $U_3<E_n<U_1$ and $U_1<E_n$, and typically a few states of electrons bound to the base region with $E_n<U_3$.

Conceptually, the simplest problem is that of a single potential step of energy U_1 in region 1 and $U_2=U_3=0$ in region 2, shown schematically in Fig. 2. To aid our discussion, we include a sketch of the probability densities $|\psi|^2$ for three types of wave functions. Wave function ψ_1 corresponds to $E_n<U_1$ and is therefore essentially zero in region 1. ψ_2 is obtained for $E_n>U_1$. Because of the lower velocity in region 1, the probability density in region 1 is larger than in region 2.[4] However, by applying the impedance matching condition for the effective electron masses m_1^* and m_2^*,[1,3]

$$E_n \simeq \frac{U_1}{1-m_1^*/m_2^*} , \tag{13}$$

the velocities a_j on either side of the barrier become equal, and there is no quantum mechanical reflection at the interface. The corresponding wave function ψ_3 therefore, has the same amplitude in both regions.

B. The electron-phonon scattering rate

An electron of initial energy E and parallel wave vector $\mathbf{k}_\parallel$ can be scattered into a final state of energy $E'=E-\hbar\omega_{\rm LO}$ and wave vector $\mathbf{k}'_\parallel=\mathbf{k}_\parallel-\mathbf{q}_\parallel$ by emission of an optical phonon of energy $\hbar\omega_{\rm LO}$ and wave vector $\mathbf{q}$. We wish to calculate the electron-phonon scattering rate $1/\tau_{n,k_\parallel}$, where $\tau_{n,k_\parallel}$ is half the lifetime of an electron in the nth subband. Adopting the low-temperature limit $(T=0)$, one finds

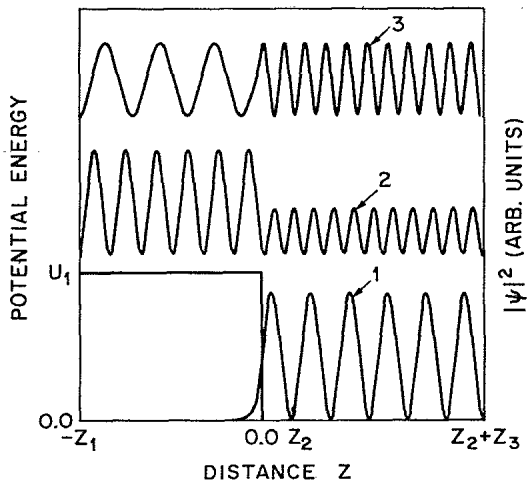

FIG. 2. Schematic potential energy diagram of an abrupt heterojunction. The potential energy in region 1 is U_1 and that in region 2 is $U_2=0$. Also shown are the probability densities of three types of wave functions.

$$1/\tau_{n,k_\parallel}=\frac{4\pi^2e^2\omega_{\rm LO}}{V\epsilon^*}\sum_{n',\mathbf{q}_\parallel,q_z}\frac{|M_{nn'}(q_z)|^2}{q_\parallel^2+q_z^2}\delta\left[E_n+\frac{\hbar^2k_\parallel^2}{2m_2^*}-E_{n'}-\frac{\hbar^2(\mathbf{k}_\parallel-\mathbf{q}_\parallel)^2}{2m_2^*}-\hbar\omega_{\rm LO}\right]. \quad (14)$$

Here, V is the volume of the system and

$$\frac{1}{\epsilon^*}=\frac{1}{\epsilon_\infty}-\frac{1}{\epsilon_0}, \quad (15)$$

where ϵ_∞ and ϵ_0 are the high- and low-frequency dielectric constants, respectively. The matrix element $M_{nn'}$ is given by

$$M_{nn'}(q_z)=\int dz\,\phi_n^*(z)e^{iq_zz}\phi_{n'}(z)\,. \quad (16)$$

We note that an analytical, but rather lengthy, expression for $1/\tau_{n,k_\parallel}$ can only be obtained for $k_\parallel=0$.

In this study, we are interested in comparing the results of calculating scattering rates in restricted heterojunction geometries with the bulk value. The bulk inelastic scattering rate $1/\tau_{\rm bulk}$ is given by[5]

$$1/\tau_{\rm bulk}=\alpha\omega_{\rm LO}\left[\frac{\hbar\omega_{\rm LO}}{E}\right]^{1/2}\ln\frac{E^{1/2}+(E-\hbar\omega_{\rm LO})^{1/2}}{E^{1/2}-(E-\hbar\omega_{\rm LO})^{1/2}}, \quad (17)$$

where α is the polaron coupling constant,

$$\alpha=\frac{e^2}{\hbar\epsilon^*}\left[\frac{m^*}{2\hbar\omega_{\rm LO}}\right]^{1/2}.$$

III. RESULTS AND DISCUSSION

A. Initial electron motion perpendicular to the heterointerfaces

We focus on GaAs/$Al_xGa_{1-x}As$ because of its widespread use as a semiconductor heterojunction. GaAs has a conduction-band effective electron mass $m^*=0.07m_0$, the optic-phonon energy is $\hbar\omega_{\rm LO}=0.036$ eV, and the high- and low-frequency dielectric constants are $\epsilon_\infty=11$ and $\epsilon_0=13$, respectively.

As a starting point, consider an electron with initial $\mathbf{k}_\parallel=0$ moving in a single-step potential similar to that shown schematically in Fig. 2. Making use of Eq. (14) we may calculate $1/\tau_{n,\,k_\parallel=0}$ as a function of electron energy E. The results of such a calculation are shown in Fig. 3 for the potential shown in the inset of the figure. Also shown as the smooth curve in the figure is the bulk-phonon scattering rate. Notice that energy conservation requires that an electron of kinetic energy $E<\hbar\omega_{\rm LO}$ cannot emit an optic phonon, so that $1/\tau_{n,\,k_\parallel=0}=0$ for $E<\hbar\omega_{\rm LO}$. An electron with energy above this threshold has a scattering rate which is similar to that of a bulk semiconductor. The small peaked deviations, which occur with increasing energy, are due to the increasing separation of energy levels. However, at $E=U_1$ the scattering rate changes abruptly from a finite value to approximately zero. Then, with increasing electron energy, $1/\tau_{n,\,k_\parallel=0}$ shows oscillatory behavior until $E>(U_1+\hbar\omega_{\rm LO})$, above which $1/\tau_{n,\,k_\parallel=0}$ again takes on the bulk value, but shifted in energy by U_1. The rapid oscillations in $1/\tau_{n,\,k_\parallel=0}$ for $U_1<E<(U_1+\hbar\omega_{\rm LO})$ are due to coherent interference arising from the existence of the infinite potential barriers used in the electron wave-function normalization procedure. We note that in a real solid interference effects of this type cannot occur over length scales greater than a characteristic mean-free path. Therefore, within this length scale, the phonon scattering rate is given by a smooth curve close to the lower bound of the oscillatory curve in Fig. 3.

An explanation of why an abrupt change in scattering rate occurs when $E=U_1$ is found by considering the electron wave functions shown schematically in Fig. 2. An electron described by a wave function ψ and having energy in the range $U_1<E<(U_1+\hbar\omega_{\rm LO})$ can only lose energy by making a transition to an electronic state ψ' which is essentially localized in region 2 in Fig. 2. Because of the spatial separation of ψ and ψ', it follows that the matrix element $M_{nn'}$ given by Eq. (16) is small, hence $1/\tau_{n,\,k_\parallel=0}$ is small in the range $U_1<E<(U_1+\hbar\omega_{\rm LO})$. In addition, due to the significant difference in electron velocity either side of the step potential, the transmission probability for an electron of energy $E\gtrsim U_1$ (see Fig. 2) is low and an electron in state ψ spends most of the time in region 1 where the potential has a value U_1.[6]

Having established what happens for the case of a simple step potential it is natural to extend our study and calculate $1/\tau_{n,\,k_\parallel=0}$ for more complicated structures.

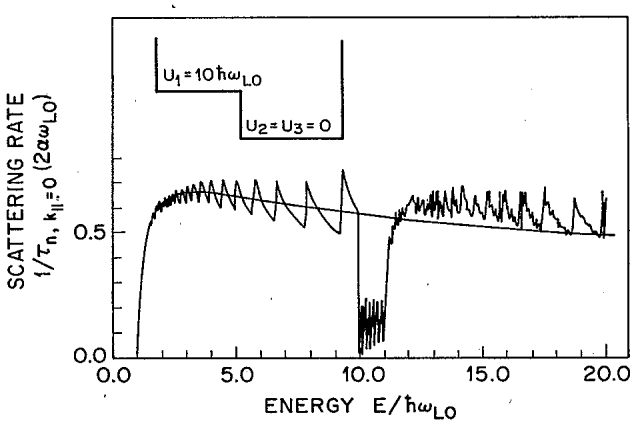

FIG. 3. Inelastic optic-phonon-scattering rate, $1/\tau_{n,\,k_\parallel=0}$, as a function of initial electron energy E. $1/\tau_{n,\,k_\parallel=0}$ is in units of $2\alpha\omega_{\rm LO}$, where α is the polaron coupling constant. The smooth curve is the bulk-phonon-scattering rate. The parameters used in the calculation were $U_1=10\hbar\omega_{\rm LO}$, $U_2=U_3=0$, $m_j^*=0.07m_0$, where m_0 is the free-electron mass, $z_2=200$ Å, and $z_1=z_3=7000$ Å.

The potential energy diagram for a typical asymmetric quantum-well unipolar-hot-electron transistor[1,3] is shown in the inset in Fig. 4(a). In this structure the emitter barrier has energy U_1, the collector barrier has energy U_3, and the transistor's quantum-well base has a width z_2. The result of calculating $1/\tau_{n,\,k_\parallel=0}$ for this geometry is shown in Fig. 4(a) and $1/\tau_{n,\,k_\parallel=0}$ for a symmetric quantum-well structure with $U_1=U_3$ is shown in Fig. 4(b). The scattering rate for electrons confined to the discrete electronic states in the transistor base is indicated with x's. Just as with the simpler case of a single potential step, there is a dramatic reduction in $1/\tau_{n,\,k_\parallel=0}$ at electron energies $E=U_1$ and $E=U_3$.

Obtaining transport properties, such as the nonequilibrium electron distribution function in transistor structures, involves finding a solution to the quantum kinetic equation for the Wigner distribution function. This is a difficult task about which we chose not to comment and instead we discuss the physical importance of our results for $1/\tau_{n,\,k_\parallel=0}$. Our data might suggest that the significant decrease in $1/\tau_{n,\,k_\parallel=0}$ for electrons with energy in the range $U_1<E<(U_1+\hbar\omega_{\rm LO})$ leads to a reduction in scattering in the transistor base and hence an increase in transistor performance. However, there is no net increase in performance due to the effect since, for *those nonequilibrium electrons injected into the base region* the scattering rate is similar to that of the bulk semiconductor. As we have already discussed, the decrease in $1/\tau_{n,\,k_\parallel=0}$ occurs because of the spatial separation of initial and final electron wave functions between emitter (region 1 in Fig. 2) and base (region 2 in Fig. 2). Because the confinement of the initial wave functions to region 1 is a direct consequence of the velocity mismatch across the abrupt change in potential, the quantum reflection at the heterojunction results in a small probability that the electrons are injected into the base. However, those that are injected scatter at a rate close to the bulk value.

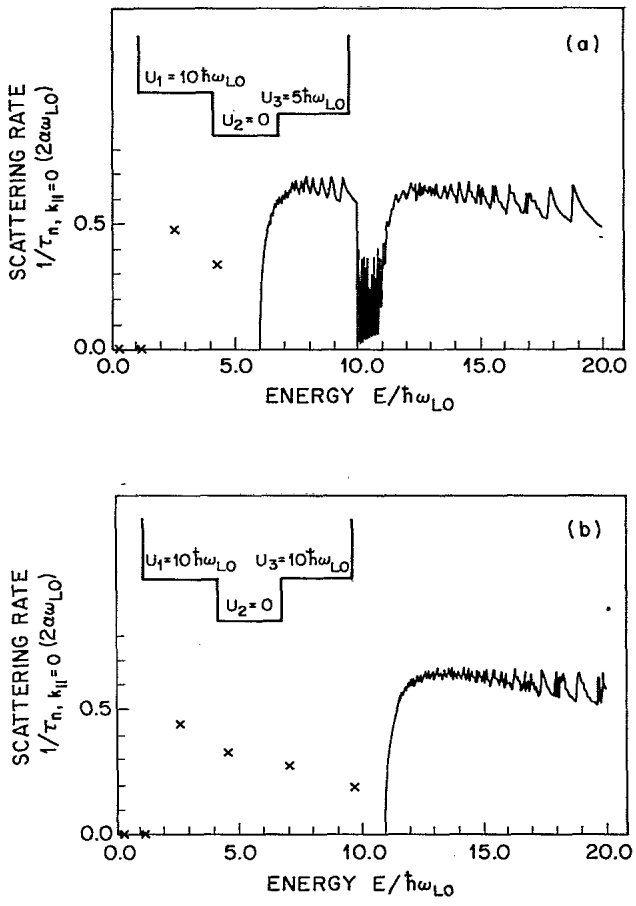

FIG. 4. (a) $1/\tau_{n,\,k_\parallel=0}$ for an asymmetric quantum-well structure with $U_1=10\hbar\omega_{\rm LO}$, $U_2=0$, $U_3=5\hbar\omega_{\rm LO}$, $m_j^*=0.07m_0$, $z_2=200$ Å, and $z_1=z_3=7000$ Å. (b) $1/\tau_{n,\,k_\parallel=0}$ for a symmetric quantum-well structure with $U_1=U_3=10\hbar\omega_{\rm LO}$, $U_2=0$, $m_j^*=0.07m_0$, $z_2=200$ Å, and $z_1=z_3=7000$ Å.

This fact may be illustrated by calculating $1/\tau_{n,\,k_\parallel=0}$ for an electron of energy E when the electron velocity in the emitter is the same as in the base (see Fig. 2). This impedance matching condition[1,3] (for which the transmission coefficient is unity) given by Eq. (13) is $m_2^*/m_1^*=E/(E-U_1)$, where m_i^* are the effective electron masses in the emitter and base, respectively. The results of calculating $1/\tau_{n,\,k_\parallel=0}$ for electrons impedance-matched at an energy $E=(U_1+\hbar\omega_{\rm LO}/2)$ are shown in Fig. 5(a). As can be seen, impedance matching has the effect of increasing the heterojunction-phonon-scattering rate to around half the bulk value because when the electron velocities are similar in region 1 and 2 the electron spends approximately half its time in region 2.

The current gain of a transistor is defined as $\beta=j_c/j_b$, where j_c and j_b are the collector and base currents, respectively. High-current gain β occurs when j_b is small. Clearly it is of interest to develop a model which estimates the energy dependence of base current in a unipolar-hot-electron transistor. We begin by considering the potential depicted in Fig. 5(b). An electron of energy E injected from the emitter side is represented by a traveling plane wave ψ. We assume that once the electron is in the collector region it contributes to the collector current. Hence, in our model, the base current is related to the base-capture rate obtained by restricting the summation in Eq. (14) to those states ψ' which are bound to the base region. In Fig. 5(b) we show the results of calculating the base-capture rate with and without impedance matching at the base-to-collector interface. In the absence of impedance matching the capture rate (dotted curve in the figure) peaks at the virtual cavity resonances of the base. Resonances of this type are detrimental to the transistor's current gain because, in the transport problem, current flows mainly via resonances where the average velocity of electrons is low and the base-capture probability is high. The effect of impedance matching at the base-to-collector junction is to smoothen the resonance characteristics by decreasing the maxima and increasing the minima in the capture rate. In the transport problem the average velocity of electrons is high and the probability of an electron contributing to base current is low. For this situation we expect the transistor's current gain to be high.

B. Initial electron motion parallel to the heterointerfaces

We now consider motion of an electron with initial wave vector parallel to the plane of the heterojunction. Understanding electron dynamics in these circumstances has direct bearing on the operation of field-effect transistors. In this case an electron is accelerated from the lowest subband in the transistor's source. Electron velocity increases parallel to a heterojunction forming the transistor gate and finally the electron is in a high-energy state in the transistor's drain.

Figure 6 shows a sketch of the electron energy E as a function of parallel wave vector $k_{\parallel}$ for the abrupt heterojunction geometry depicted in the inset. Also shown are the scattering processes an electron accelerated in the lowest subband $n=1$ can undergo. The scattering rate

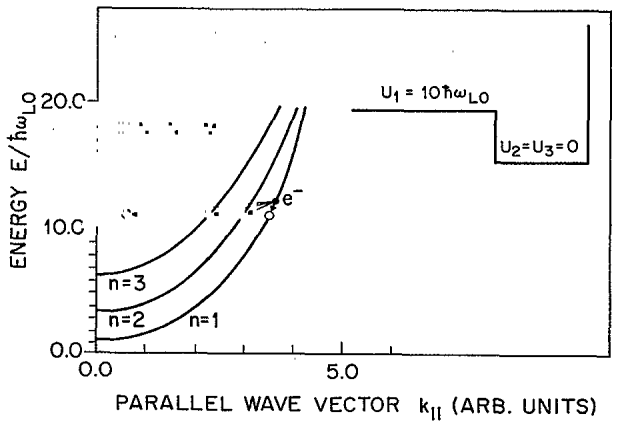

FIG. 6. Schematic diagram of electron energy E plotted as a function of parallel wave vector $k_{\parallel}$ for the heterojunction geometry depicted in the inset. Also shown are the scattering processes an electron in the lowest subband can undergo.

$1/\tau_{n=1,\,k_{\parallel}}$ for this geometry is shown in Fig. 7 as a function of initial electron energy E. The result is close to the bulk curve, except for the discontinuities occurring at the energies $E=E_n+\hbar\omega_{\mathrm{LO}}$. At these energies scattering into the subsequent subbands becomes possible, i.e., additional scattering channels open up. The discontinuities become smaller with increasing energy E, because—as evident from Fig. 6—increasing momentum transfers $\mathbf{q}$ are involved and large-$|\mathbf{q}|$ values only make small contributions to $1/\tau_{n,k_{\parallel}}$ [see Eq. (14)]. For the same reason and in contrast to $k_{\parallel}=0$ injection above U_1, almost no effect shows up for $n=1$ in the energy range $U_1<E<U_1+\hbar\omega_{\mathrm{LO}}$. The dashed line in Fig. 7 gives $1/\tau_{n=1,\,k_{\parallel}}$, but with the final states restricted to $E_n'<U_1$. Obviously, there is only little difference to the full result, i.e., "real-space transfer" out of the well is not very important, at least for energies close to U_1.

In Fig. 8(a) is shown again $1/\tau_{n=1,\,k_{\parallel}}$ for the same geometry, while 8(b) shows $1/\tau_{n,k_{\parallel}}$ for an electron in the

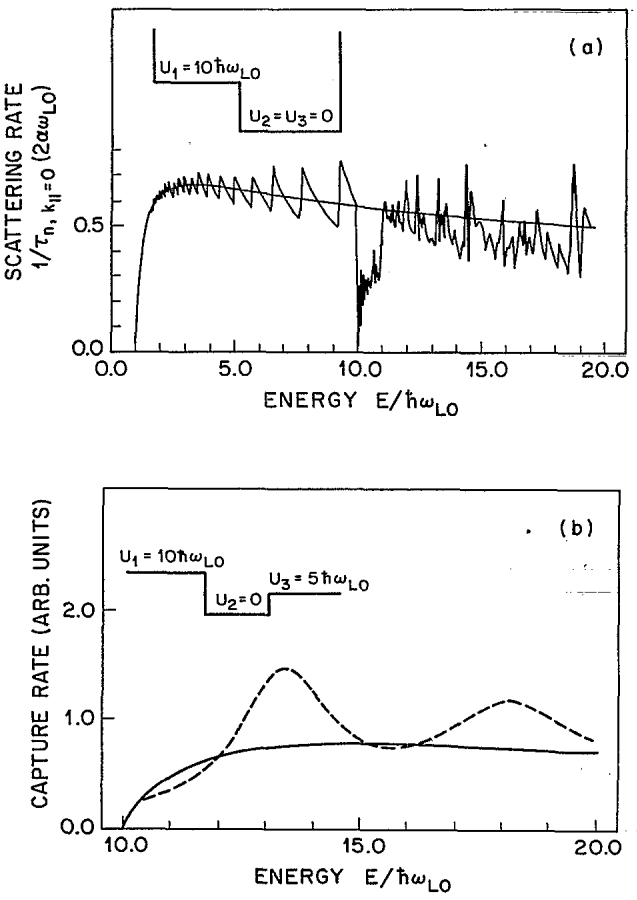

FIG. 5. (a) $1/\tau_{n,\,k_{\parallel}=0}$ for a heterojunction impedance matched at an electron energy $E=10.5\hbar\omega_{\mathrm{LO}}$. The smooth curve is the bulk-phonon-scattering rate. The parameters used in the calculation were $U_1=10\hbar\omega_{\mathrm{LO}}$, $U_2=0$, $m_1^*=0.0476m_2^*$, $m_2^*=0.07m_0$, $z_2=200$ Å, and $z_1=z_3=7000$ Å. (b) Base-capture rate as a function of initial electron energy for an asymmetric quantum-well structure. The dotted line corresponds to an impedance-mismatched base-to-collector junction with $m_3^*=10m_2^*$. The solid line corresponds to impedance matching with $m_3^*=0.68m_2^*$. The other parameters used in the calculation were $U_1=10\hbar\omega_{\mathrm{LO}}$, $U_2=0$, $U_3=5\hbar\omega_{\mathrm{LO}}$, $m_2^*=0.07m_0$, $z_2=200$ Å, and $z_1=z_3=7000$ Å.

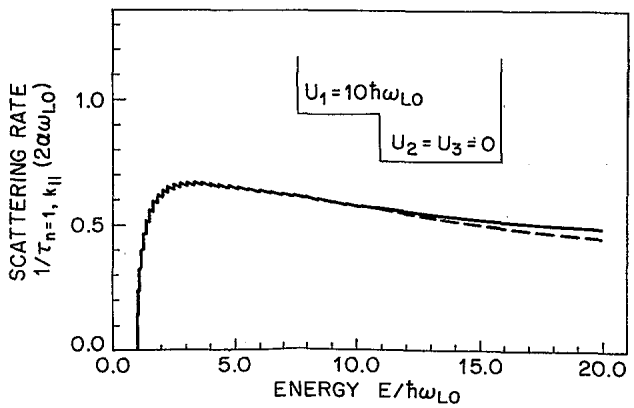

FIG. 7. $1/\tau_{n=1,\,k_{\parallel}}$ as a function of initial electron energy E. The dashed line gives $1/\tau_{n=1,\,k_{\parallel}}$ with the final states restricted to $E_n'<U_1$. The parameters used in the calculation were $U_1=10\hbar\omega_{\mathrm{LO}}$, $U_2=U_3=0$, $m_j^*=0.07m_0$, $z_2=200$ Å, and $z_1=z_3=1000$ Å.

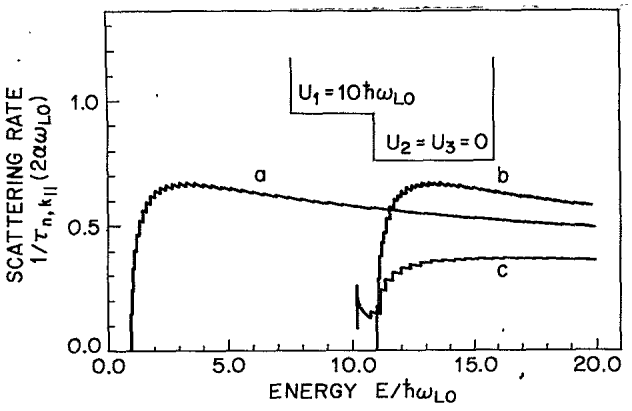

FIG. 8. (a) Same as solid line in Fig. 7. (b) $1/\tau_{n,k_\parallel}$ for an electron in the lowest subband above U_1. (c) Same as (b) but with impedance matching at $E=11\hbar\omega_{LO}$ ($m_1^*=m_2^*/11$).

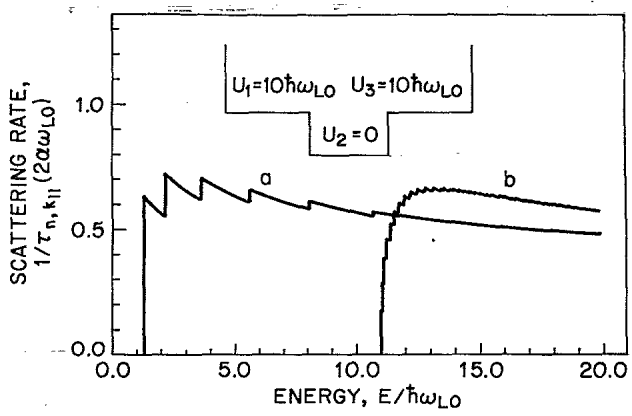

FIG. 10. $1/\tau_{n,k_\parallel}$ for a symmetric quantum-well structure with $U_1=U_3=10\hbar\omega_{LO}$, $U_2=0$, $m_j^*=0.07m_0$, $z_2=200$ Å, and $z_1=z_3=1000$ Å. (a) $1/\tau_{n=1,k_\parallel}$. (b) $1/\tau_{n,k_\parallel}$ for an electron in the lowest subband above U_1.

lowest subband above U_1. The latter is again close to the bulk value, but shifted in energy by U_1. In addition, the scattering rate is essentially zero for $U_1<E<U_1+\hbar\omega_{LO}$, because the initial state is localized on the left site of the interface, while for this energy region scattering is only possible into states with $E_n'<U_1$, which are localized on the right side, as discussed above. Figure 8(c) again shows the scattering rate for the lowest subband above U_1, but the effective mass m_1^* was now chosen to be $m_1^*=m_2^*/11$, so that according to Eq. (13) impedance matching occurs at $E=11\hbar\omega_{LO}$. The effect of the impedance matching is substantial. There is now a finite-scattering rate for $U_1<E<U_1+\hbar\omega_{LO}$, since the initial state is extended over the whole device, while for $U_1+\hbar\omega_{LO}<E$ the bulk-scattering rate corresponding to the reduced density of states is approached. The effect of impedance matching on $1/\tau_{n=1,k_\parallel}$ is negligible because real-space transfer is not important, as discussed above.

Figures 9 and 10 show the scattering rates for asymmetric and symmetric hot-electron-transistor structures with equal effective electron masses in the emitter, base, and collector, respectively. Figures 9(a) and 10(a) are for electrons in the lowest, $n=1$, subband, 9(b) and 10(b) for electrons in the lowest subband above U_3, and 9(c) for an electron in the lowest subband above U_1. In all cases, the overall behavior is similar to that of the bulk-scattering rate, except for (i) shifts by the potential discontinuities and (ii) nearly collision-free regions $U_i<E<U_i+\hbar\omega_{LO}$.

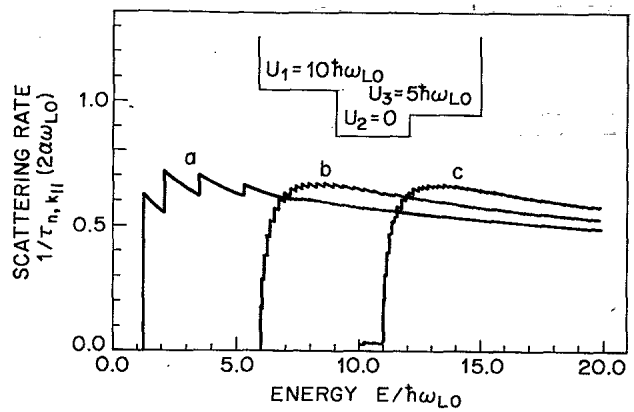

FIG. 9. $1/\tau_{n,k_\parallel}$ for an asymmetric quantum-well structure with $U_1=10\hbar\omega_{LO}$, $U_2=0$, $U_3=5\hbar\omega_{LO}$, $m_j^*=0.07M_0$, $z_2=200$ Å, and $z_1=z_3=1000$ Å. (a) $1/\tau_{n=1,k_\parallel}$. (b) $1/\tau_{n,k_\parallel}$ for an electron in the lowest-subband above U_3. (c) $1/\tau_{n,k_\parallel}$ for an electron in the lowest subband above U_1.

IV. CONCLUSIONS

In conclusion, quantum mechanical reflection at an abrupt semiconductor heterojunction can localize initial and final electron states on either side of the junction. For an electron with initial $k_\parallel=0$, this spatial separation, due to scattering from a potential step, strongly reduces inelastic polar-optic-phonon-scattering rates for a limited range of electron energies. However, the influence of this phenomenon on the current gain of hot-electron transistors is small, because the increase in scattering time is canceled by the decrease in transmission probability. Neglect of this phenomenon will cause significant errors in device modeling. We have also demonstrated that resonances in electron-scattering rates may be removed by impedance matching electron states across the base-to-collector junction. The removal of these resonances should increase the current gain of unipolar-hot-electron transistors.

Scattering rates for an electron with all its initial momentum parallel to the heterojunction's plane are little changed by the presence of the heterojunction. This is because the probability of large-angle scattering (large-$|\mathbf{q}|$ transfers) is small. As a result, the inelastic scattering of hot electrons by polar-optic phonons in a field-effect transistor will not result in significant transfer of electrons into states spatially localized above the barrier. This should not be confused with the real-space transfer introduced by Hess and co-workers,[7] which involves different scattering mechanisms.

*Permanent address: Institut für Theoretische Physik, Universität Frankfurt, Robert-Mayer-Strasse 8, D-6000 Frankfurt-am-Main 1, West Germany.

[1]A. F. J. Levi and T. H. Chiu, Appl. Phys. Lett. **51**, 984 (1987).

[2]F. A. Riddoch and B. K. Riddley, Physica B **134**, 342 (1985).

[3]J. F. Müller, S. Schmitt-Rink, and A. F. J. Levi, Appl. Phys. Lett. **52**, 236 (1988).

[4]L. D. Landau and E. M. Lifshitz, *Quantum Mechanics* (Pergamon, Oxford, 1981).

[5]E. M. Conwell, in *Solid State Physics, Advances in Research and Applications,* edited by H. Ehrenreich, F. Seitz, and D. Turnbull (Academic, New York, 1967), Vol. 9, p. 156.

[6]Dissipative processes, such as phonon scattering, are expected to effect this transmission probability. See, e.g., R. Bruinsma and P. M. Platzman, Phys. Rev. B **35**, 4221 (1987).

[7]K. Hess, H. Morkoc, H. Shichijo, and B. G. Streetman, Appl. Phys. Lett. **35**, 469 (1979); K. Hess, J. Phys. (Paris), Colloq. **42**, C7-3 (1981).